Express Polymer Letters Vol.18, No.6 (2024) 561–574
Available online at www.expresspolymlett.com
https://doi.org/10.3144/expresspolymlett.2024.42

Research article

Dielectric elastomers based on SEBS gel: The impact of adding kraft lignin on electro-mechanical performance

*Rogerio Ramos de Sousa Junior, Guilherme Elias Saltarelli Garcia, Leonardo Dalseno Antonino, Júlia Rocha Gouveia, Demetrio Jackson dos Santos, Danilo Justino Carastan**

Center for Engineering, Modeling and Applied Social Sciences Federal University of ABC (UFABC), Av. dos Estados, 09210-580 Santo Andre, Brazil

Received 20 January 2024; accepted in revised form 9 March 2024

Abstract. Thermoplastic elastomer gels based on styrenic triblock copolymers have been increasingly used as dielectric elastomers, particularly due to the possibility of tailoring their properties based on their composition. However, these materials have a low relative permittivity, primarily attributed to their low dipole moment. Consequently, this characteristic poses a challenge for their application as dielectric elastomers. In this work, we aim to assess the impact of adding kraft lignin on the dielectric properties of thermoplastic elastomer gels. Additionally, we investigate the effects of kraft lignin dispersion on their viscoelastic and mechanical properties. For this purpose, we used two types of kraft lignin: acidic and alkaline (ac-KL and alk-KL). The alk-KL demonstrated higher dispersibility in the polymer, mainly attributed to the deprotonation of its structure during its production process. As a result, the dielectric elastomer with alk-KL showed a 50% increase in relative permittivity compared to the pristine polymer without compromising its mechanical and viscoelastic properties. Moreover, these samples demonstrated a greater actuation strain capability in response to an electrical stimulus. Thus, the incorporation of lignin demonstrates promise as a valuable reinforcement in the development of advanced dielectric materials, enhancing their electro-mechanical performance.

Keywords: *thermoplastic elastomer, block copolymer, kraft lignin, electroactive polymer, dielectric properties*

1. Introduction

Electroactive polymers (EAPs) are a class of smart materials that respond to an external electrical stimulus with movement and/or mechanical deformations, making them suitable for a variety of applications, including soft robots, sensors, and actuators [1–4]. They are often referred to as artificial muscles [4] due to their ability to exhibit controlled mechanical responses, even on a small scale. Among EAPs, dielectric elastomers (DEs) are the category most analogous to artificial muscles [4, 5]. Consequently, DEs have been the subject of significant research and technological efforts in recent years [3–5].

Typically, the conversion of electrical into mechanical energy is facilitated by a dielectric elastomer actuator (DEA), which consists of a dielectric membrane with compliant electrodes. An electrical stimulus charges the electrodes, leading to compressive loading on the dielectric membrane due to coulombic attraction, referred to as Maxwell stress (σ_M). As the dielectric elastomer undergoes compression, its area expands proportionally, a result of the material's incompressible nature [4, 5]. Electro-mechanical performance can be quantified by its actuation strain (S_Z), according to Equation (1) [6]:

$$S_z = \frac{\sigma_M}{Y} = \frac{\varepsilon'\varepsilon_0 E_f^2}{Y} = \frac{\varepsilon'\varepsilon_0}{Y}\left(\frac{V}{z}\right)^2 \quad (1)$$

*Corresponding author, e-mail: danilo.carastan@ufabc.edu.br

where σ_M is the Maxwell stress, Y is the compressive modulus, ε' is the relative permittivity of the elastomer, ε_0 is the permittivity in vacuum, E_f is the electric field, V is the voltage, and z is the thickness of the material.

Consequently, properties such as low elastic modulus, combined with large strains and high relative permittivity, are crucial for dielectric elastomer membranes. These properties allow for larger mechanical strain, even under low-intensity electric fields (reduced voltage in the electrodes) [3]. In this context, thermoplastic elastomer gels (TPEGs) emerged as promising materials for dielectric elastomers [5]. Most of these polymer gels are composed of a styrenic triblock copolymer, comprising a central rubbery block with two polystyrene (PS) end-blocks [7–10]. TPEGs can be produced by incorporating a low-volatility organic solvent with selective interaction with the rubbery block [8, 10]. In the gel state, the midblock forms a three-dimensional swollen structure, while the endblocks associate to form aggregates in a spherical structure [9, 11]. Although TPEGs meet the mechanical criteria for dielectric elastomer applications, they exhibit a low dipole moment and, like most polymer materials, a low relative permittivity [8].

In this context, strategies such as obtaining nanocomposites and polymer blends are commonly employed to enhance the relative permittivity in DEs [3]. Bolados *et al*. [12] developed blends of polystyrene-*b*-poly(ethylene-butylene)-*b*-polystyrene (SEBS) and thermoplastic polyurethane (TPU) at various concentrations, aiming to combine the favorable processability and flexibility of SEBS with the higher relative permittivity of TPU. The optimal electromechanical performance was achieved by adding 10 wt% of TPU to the SEBS matrix. While higher concentrations of TPU led to greater relative permittivities, they also caused more pronounced matrix stiffening, compromising the required balance between relative permittivity and elastic modulus.

Another approach involves incorporating conductive nanomaterials into DEs to impart higher relative permittivities to the systems. The concentration and particle size of the nanomaterials are carefully determined to ensure that the systems remain below the percolation threshold. This is a condition where the relative permittivity experiences a significant increase despite an increase in dielectric loss. Additionally, high relative permittivity ceramics can be integrated into dielectric elastomer matrices to substantially elevate the relative permittivity of the systems. However, the addition of ceramics renders DEs more susceptible to dielectric breakdown. Studies have evaluated the effects of concentration [13–17], functionalization [14–18], and dispersion [14, 15, 19, 20] of these nanomaterials on the dielectric properties of polymer matrices.

For instance, Chen *et al*. [13] incorporated up to 1.2% of exfoliated graphene nanoplatelets in polystyrene-*b*-polybutadiene-*b*-polystyrene (SBS). Impedance analysis revealed a significant increase in the relative permittivity near the percolation threshold (15.96 for the 1.19%-loaded sample compared to 2.72 for the pure SBS at a frequency of 1 kHz). However, the results also showed a notable increase in dielectric loss, which was attributed to current leakage and might pose challenges for the material's application in DEs. McCarthy *et al*. [17] employed SEBS and titanium dioxide (TiO_2) nanoparticles, both with and without functionalization, to regulate the nanoparticle and polymer interfacial interaction. The results demonstrated a proportional increase in permittivity with nanoparticle concentration, with an optimal TiO_2 concentration of 5 vol%. Beyond this concentration, increased stiffness hindered the application of the materials as DEA.

In this context, lignin emerges as a promising and underexplored alternative to enhance the relative permittivity in TPEGs. Lignin's structure may exhibit high polarizability [21] due to the aromatic backbone and a wide array of functional groups, including aliphatic and phenolic hydroxyls, methoxyls carbonyls, and carboxyls, as exemplified in Figure 1. In addition, lignin is a biopolymer abundantly available. Accounting for 15 to 40% of the composition of trees, plants, and algae, it is the most abundant naturally occurring aromatic polymer [22, 23]. Lignin possesses complex and amorphous three-dimensional structures originating from the polymerization of three aromatic alcohol precursors (monolignols): coniferyl, sinapyl, and *p*-coumaryl alcohol [24, 25]. It should be noted that technical lignins, obtained through industrial pulping processes, are readily available for utilization. Of particular significance is the lignin derived from the kraft pulping process, which is a byproduct of the widely employed kraft pulping process in the paper and cellulose industry, yielding approximately 130 Mt annually [26, 27].

Lignin has been employed as a reinforcing agent in polymer matrices, imparting properties such as

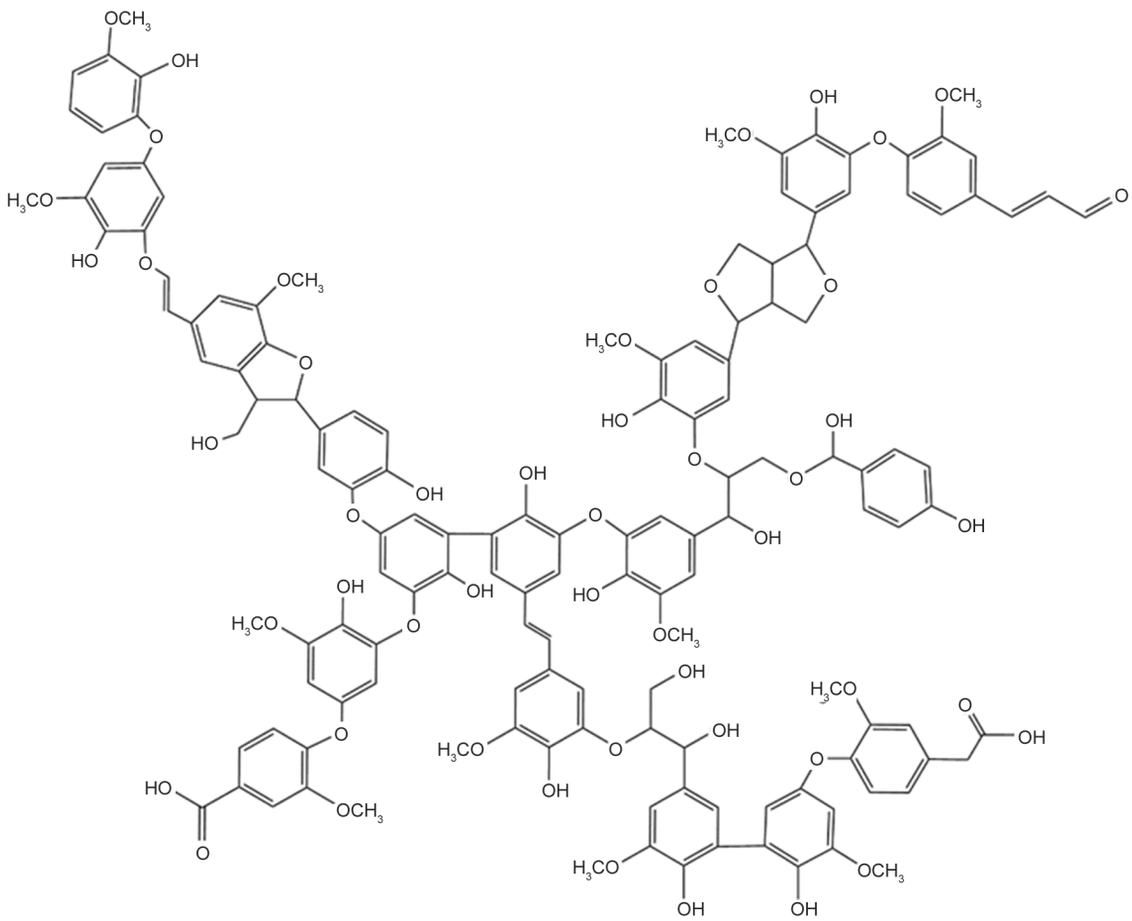

Figure 1. Representative structure of a lignin.

antioxidants, flame retardants, or reinforcement fillers [28]. However, due to its polar structure and tendency to form clusters within polymeric matrices, attributed to strong intra and intermolecular bonds [28], achieving high-performance composites significantly hinges on achieving an appropriate dispersion of the lignin within the polymer matrix, impacting the properties of the resulting materials.

In elastomers applied as smart polymers, Stiubianu *et al*. [29] explored the potential of lignin as a reinforcement in a polysiloxane matrix. To enhance the lignin-polymer interaction, they carried out lignin modification through an allylation reaction, resulting in a composite with increased relative permittivity and low elastic modulus. These properties allow for applications such as energy harvesting and electromechanical actuation. Zhang *et al*. [30] proposed a composite using an ionomeric elastomer with the addition of unmodified lignin, where the incorporation of zinc oxide improved compatibility between the components, resulting in a fine dispersion of lignin in the elastomer matrix and excellent mechanical properties. The obtained elastomer was evaluated as a shape memory material, demonstrating a shape recovery ratio of 88%. In this work, we propose the use of unmodified kraft lignin, thereby eliminating a processing step compared to previously published works, while evaluating the pH difference in these lignins as mechanisms to achieve better dispersion in TPEG.

Thus, we aim to assess the impact of adding kraft lignin (KL) to SEBS block copolymer-based polymeric gels used as dielectric elastomers. Specifically, two lignins, differing in their pH levels (3.5 or 8.1), were employed. The resulting composites were characterized by their mechanical, viscoelastic, and dielectric properties, mainly based on the lignin dispersion. Consequently, we proposed a straightforward approach to enhance the electro-mechanical performance of DEs by elevating the relative permittivity without a significant increase in the elastic modulus. Dielectric elastomers produced with the higher pH kraft lignin, called alk-KL, exhibited a finer dispersion within the polymer matrix, resulting in a lower elastic modulus with greater strain capacity, as well as a higher relative permittivity compared

to the addition of kraft lignin with lower pH, named as ac-KL. These attributes enabled a superior electro-mechanical performance in the composites with an addition of up to 5 wt% of alk-KL. The findings of this study may contribute to the advancement of dielectric elastomers utilized in applications such as artificial muscles, particularly in soft robotics, allowing for improved mechanical response in a reduced electric field. Additionally, our utilization of kraft lignin holds broader implications. Serving as a cost-effective and readily available natural polymer, it emerges as a compelling alternative to fossil-based materials.

2. Materials and methods

2.1. Materials

Polystyrene-*b*-poly(ethylene-*co*-butylene)-*b*-polystyrene (SEBS) block copolymer (Kraton G1652), with 30 wt% of polystyrene block, was kindly supplied by Kraton (Paulínia, Brazil). White mineral oil (MO) was acquired from DinTables âmica (Diadema, Brazil), and the hydrogenated hydrocarbon resin (HCR - Sukorez SU120) was provided by Kolon Industries (Seoul, South Korea). Laboratory grades of kraft lignins (KL) from eucalyptus, with different pHs (ac-KL, pH = 3.5 and alk-KL, pH = 8.1), were kindly supplied by Suzano S.A. (Limeira, Brazil). The main characteristics of the raw materials used are described in Tables 1 and 2. The molecular weight of the block copolymer (Table 1) was obtained by gel permeation chromatography (GPC) [31], and total hydroxyl (OH) values of both lignin samples (Table 2) were obtained by phosphorus-31 nuclear magnetic resonance (^{31}P NMR) [32]. The additional data presented in Tables 1 and 2 represent information provided by the manufacturers.

Table 1. Properties of raw materials used to obtain TPEG.

Block copolymer			
Material	**Density, ρ [g/cm^3]**	**M_w [g/mol]**	**Polydispersity index M_w/M_n**
SEBS	0.91	79 000	1.04
Oligomers			
Material	**Density, ρ [g/cm^3]**	**M_w [g/mol]**	**Viscosity 40 °C [m^2/s]**
MO	0.84	N/A	$1.2 \cdot 10^{-5}$
HCR	1.08	570	N/A

Table 2. Properties of kraft lignin samples.

Kraft lignin	pH	M_w [g/mol]	OH [mmol/g]	Ash content [%]
ac-KL	3.5	2595	5.61	2
alk-KL	8.1	2829	5.14	2

2.2. TPEG preparation

TPEGs were obtained through a solution process using toluene as solvent. The mixture of the polymer gel components (SEBS, MO, and HCR) was conducted using magnetic stirring at 60 °C for 2 h. Subsequently, the solution was poured into a Petri dish and kept in an exhaust hood for 7 days to allow for solvent evaporation. Afterward, the obtained materials were placed in a vacuum oven overnight at 50 °C. The basic composition of the gels was 30 vol% SEBS, 20 vol% MO, and 50 vol% HCR. These concentrations were based on prior work by the group, which assessed the mechanical stability and deformability of these polymeric gels as a function of component concentration [33]. The incorporation of lignin into SEBS gels was carried out in the molten state using a Plastograph EC torque rheometer equipped with a W50ET mixer (Brabender, Duisburg, Germany). The SEBS gels were maintained at 80 °C for 5 min, followed by the addition of lignin (concentrations of 1, 5, 10, and 15 wt%.) for an additional 5 min. Finally, the formed samples were pressed in a heated hydraulic press at 80 °C and 0.5 MPa to uniform the thickness and morphology of the samples. Samples obtained were designated as XX ac-KL or alk-KL, where XX denotes the concentration of lignin.

2.3. TPEG characterization

Optical microscopy was used to investigate the dispersion of KL in the polymer matrix. Micrographs were captured in transmission mode using an optical microscope (Carl Zeiss Axio Scope A1, Oberkochen, Germany) equipped with a heating stage (Linkam T95 HS, Salfords, United Kingdom). For this, a small portion of the sample was compressed between two glass slides at a temperature of 90 °C. The average size of aggregates was determined by measuring at least 20 aggregates for each sample, utilizing the ImageJ software.

Dynamic mechanical analysis (DMA) was conducted on a DMA Q800 equipment (TA instruments, Waltham, United States) to assess the variation of viscoelastic characteristics of TPEG in response to the addition of KL. Rectangular samples, with dimensions of 30×8×1.2 mm, were subjected to tension

mode analysis at a frequency of 1 Hz and a strain amplitude of 10 μm. The testing temperature was set from 100 up to 80 °C with a heating ramp of 3 °C/min. The mechanical properties of the samples were evaluated through uniaxial tensile and compressive tests. Tensile tests were conducted using universal mechanical testing equipment (Instron/Emic 23-20, Norwood, United States), equipped with a 10 N load cell, and operated at a displacement rate of 5 mm/min. Rectangular samples with dimensions of 30×6.5×0.8 mm were utilized. Compression tests were performed on a rotational rheometer (Anton Paar MCR502, Graz, Austria), where 8 mm wide, 1 mm thick disks were compressed between two 25 mm parallel plates. In this setup, a normal force sensor with a maximum capacity of 40 N was employed. The displacement rate was set at 0.1 mm/min, and to mitigate shear forces during the test, a thin layer of silicone grease was applied to both plates for each specimen.

The relative permittivity (ε′) values were obtained at room temperature using an impedance analyzer (Solartron 1260, Leicester, United Kingdom) coupled with a dielectric interface (Solartron 1296, Leicester, United Kingdom). The measurements utilized a parallel plate sample holder with disk-shaped samples, each having a diameter of 20 mm and a thickness of 1 mm. The frequency sweep ranged from 10^5 to 10^{-1} Hz with a voltage set at 3 V.

The electro-mechanical experiments were conducted on a circular dielectric actuator. A film of TPEG with KL, initially measuring 60 mm in diameter and 0.9 mm in thickness, underwent 150% biaxial prestretching and was affixed to a circular rigid frame. Each surface of the dielectric actuator was coated with a compliant electrode fabricated from a mixture of silicone grease and carbon nanotubes, covering a circular area constituting up to 2% of the total membrane surface. This covered area is considered the active region, representing the zone of interest that will induce mechanical strain in response to the applied electric field, while the remaining portion of the membrane serves as the passive area. The application of an electric field results in the actuation pressure compressing the membrane thickness, which leads to an expansion of the active area, as depicted in Figure 2.

Electro-mechanical actuation was initiated by applying a voltage gradient at a rate of 0.5 kV every 5 s until the dielectric breakdown occurred. The voltage supply was provided by a high-voltage source

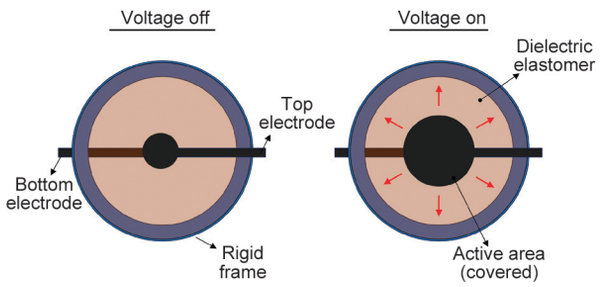

Figure 2. Dielectric elastomer actuation test setup.

(Phywe, Göttingen, Germany), and the monitoring of actuation strain was carried out through video capture at a frame rate of 60 frames per second. Subsequent frame-by-frame analysis was conducted utilizing the ImageJ software, and the actuation strain was calculated considering the incompressibility of the elastomeric gel.

3. Results and discussion

3.1. Dispersion of KL

First, it is important to emphasize that the procedure used to disperse lignin into the polymer matrix through shear in the molten state has proven to be a suitable technique [30, 34, 35]. Figure 3 presents optical micrographs of TPEG with different concentrations of ac-KL (Figure 3a–3c) and alk-KL (Figure 3d–3e). Differences in the dispersion of each KL sample can be clearly noted. The addition of ac-KL, even at lower concentrations, tends to form clusters distributed in the TPEG matrix. Sample 1 ac-KL (not shown here) exhibits large aggregates, with an average size of 56±32, up to 213 μm in some regions. By increasing the concentration of ac-KL, the average aggregate size exhibits an upward trend, measuring 66±55, 65±71, and 82±61 μm for samples containing 5, 10, and 15% ac-KL, respectively (see Figure 3a–3c). Aggregates as large as 370 μm can be seen in sample 15 ac-KL (Figure 3c). In contrast, composites incorporating alk-KL demonstrate a more refined dispersion within the TPEG matrix. Across concentrations up to 10% alk-KL, the average aggregate size remains around 15 μm, with only sample 15 alk-KL (Figure 3f) exhibiting slightly larger aggregates, measuring an average of 27 μm. For samples containing alk-KL, due to the challenge of determining the sizes of more uniformly dispersed aggregates, performing a statistical analysis is not feasible.

Despite the difference in polarity between TPEG's nonpolar composition and KL's polar structure, a significant interaction could emerge due to KL's

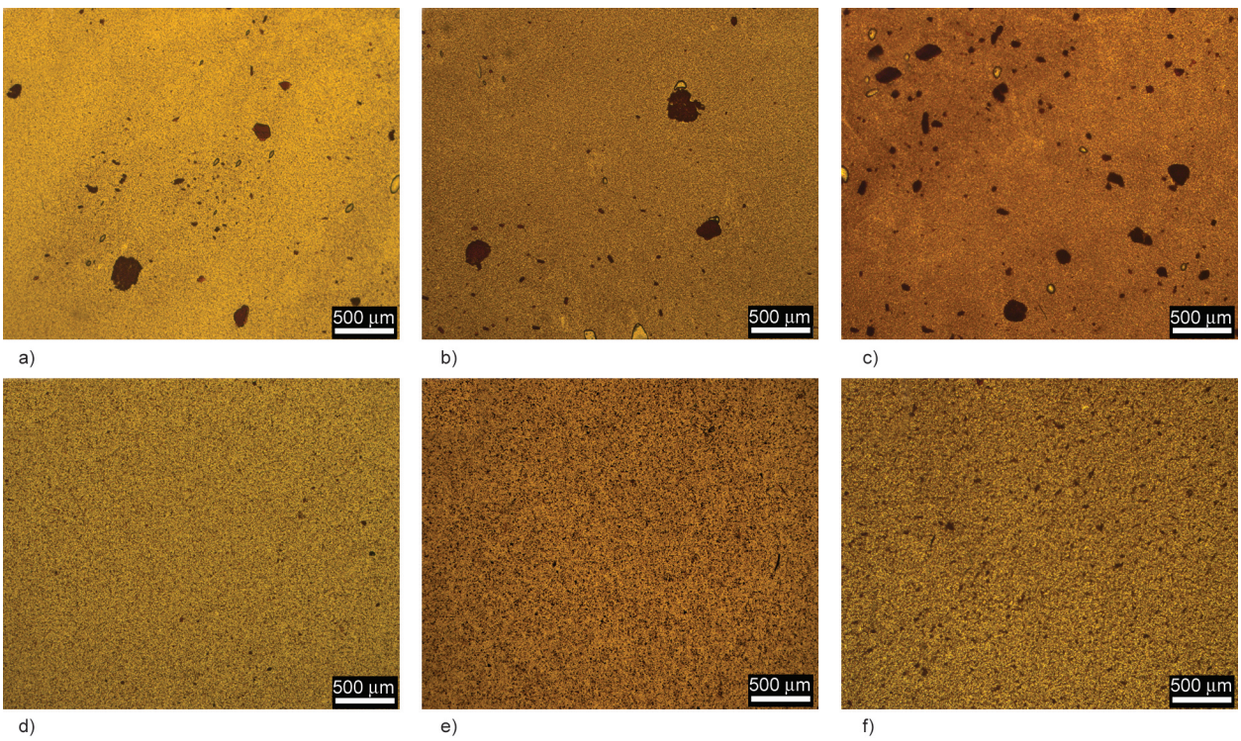

Figure 3. Optical micrographs of TPEG with KL: concentrations of 5, 10, and 15 wt% of ac-KL (a–c) and alk-KL (d–f).

strong affinity for structures containing aromatic rings, like polystyrene. These interactions are relatively weak, but they should contribute to enhanced compatibility between the lignin aromatic structure and the PS-rich phase by forming π-π stacking interactions [36, 37]. However, the results revealed different behaviors associated with each type of added lignin despite the shared high concentration of aromatic rings in both lignin varieties. In this context, another reason must be proposed to elucidate the better performance presented by alkaline lignin.

The variation in dispersion between ac-KL and alk-KL might be explained by considering the differences in the degree of deprotonation of each lignin isolated at different pH levels. Alkaline lignin possesses a higher deprotonation degree in comparison with its acidic counterpart [38, 39]. This is because alk-KL is obtained at an earlier stage of the acidification process (Lignoboost®), leading to negatively charged lignin fragments [39, 40]. These negative charges might generate electrostatic repulsive forces among alk-KL molecules, which inhibit the agglomeration of lignin particles. Consequently, the electrostatic repulsion between lignin molecules in alkaline conditions hinders the phenomena of agglomeration and particle aggregation. On the other hand, a reduction in pH through acidification leads to the protonation of previously negatively charged lignin sites. This neutralizes the negative charges, facilitating the aggregation of ac-KL particles. Then, ac-KL exhibits a higher tendency to form aggregates than alk-KL since lignin-lignin interactions are stronger than lignin-gel interactions for the former. A model illustrating the types of interactions between TPEG and each lignin sample is proposed in Figure 4.

3.2. Viscoelastic behavior

Figure 5 presents the DMA curves of the analyzed composites, showing the storage modulus (E' – Figure 5a) and the damping factor ($\tan\delta$ – Figure 5b) of samples with ac-KL and alk-KL. From the E' curves (Figure 5a), it can be observed that the addition of both KL samples does not significantly change the viscoelastic behavior of the gels. However, there is a slight extension of the glassy plateau at sub-ambient temperatures, indicating an increase in the rubbery matrix's T_g, as will be discussed further with the assistance of the $\tan\delta$ curves. Additionally, in the rubbery plateau, which corresponds to the temperature range between 30 to 60 °C, a slight increase in the E' value proportional to the KL concentration is noticeable. This increase may be due to the higher structural rigidity of KL [41, 42] as well as the possibility of KL acting as a potential site for physical cross-linking in the structure [43], resulting in an increased rubbery plateau.

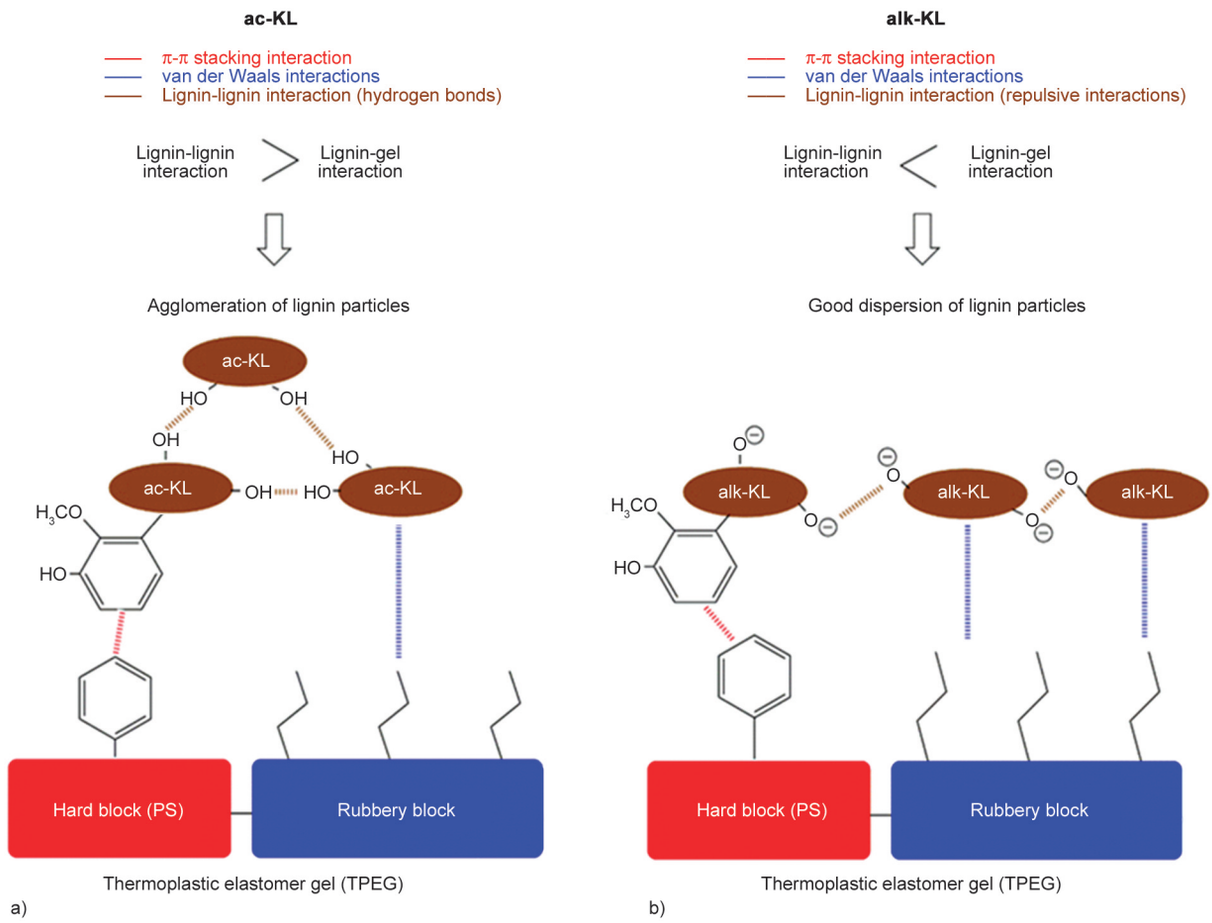

Figure 4. Scheme of lignin-lignin and lignin-TPEG interactions showing the difference in dispersion of a) ac-KL and b) alk-KL.

The peak of tan δ (Figure 5b) is associated with the glass-transition temperature (T_g) of the rubbery phase of the polymer matrix. A T_g value of 4 °C was obtained for pristine TPEG.

It is important to note that typically SEBS exhibits a sub-ambient T_g related to the rubbery block ($T_g \approx$ –50 °C) and a second T_g related to the PS end blocks ($T_g \approx$ 100 °C). In this work, other components of TPEG composition (MO and HCR) selectively interact with the rubbery block [33]. It is well-established that MO has a plasticizing effect on SEBS [9, 11]. On the other hand, HCR imposes mobility restrictions on the flexible segment, resulting in an increase in T_g [44]. At last, the low volumetric fraction of the PS end blocks causes a premature flow characteristic of the material, where a transition from

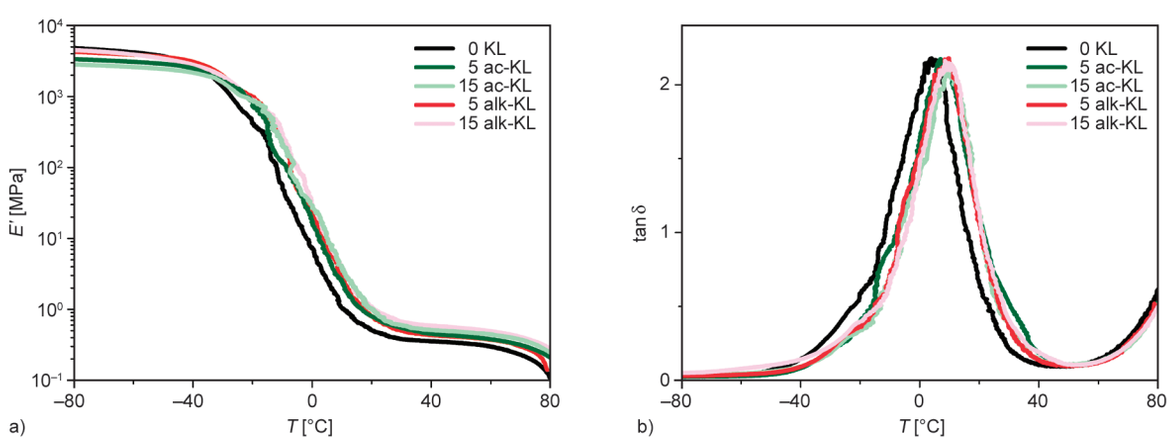

Figure 5. DMA curves: a) storage modulus and b) tan δ.

Table 3. Values of T_g and storage modulus (E') from DMA.

Sample	T_g [°C]	E' at 40 °C [MPa]
TPEG	4.11±0.26	0.39±0.02
1 ac-KL	8.23±0.56	0.44±0.02
5 ac-KL	8.05±1.04	0.39±0.07
10 ac-KL	8.54±1.46	0.54±0.03
15 ac-KL	7.90±0.79	0.60±0.09
1 ac-KL	9.50±0.40	0.49±0.06
5 ac-KL	10.58±0.95	0.46±0.03
10 ac-KL	8.32±1.80	0.53±0.02
15 ac-KL	9.39±0.89	0.61±0.02

predominantly elastic to viscous response begins from 65 °C, preventing the acquisition of the T_g related to the PS end blocks [33, 45].

With the addition of KL, regardless of type or concentration, the T_g value ranges between 8 and 10 °C. This increase in T_g is associated with the restriction of polymer chain mobility due to the presence of KL [46]. The complex branched structure of KL hinders the structural mobility of the polymer matrix, thus increasing its T_g.

It is interesting to note that both the value of the elastic modulus in the rubbery plateau and the T_g – considered as the temperature belongs to the maximum value of the tan δ – are influenced by the presence of KL and not by the formation of larger aggregates as in the samples with ac-KL. The T_g and storage modulus values in the glassy plateau region (E' at 40 °C) are presented in Table 3 for all samples.

3.3. Mechanical properties

The results obtained from the mechanical tensile and compression tests are shown in Figure 6 as a function of the concentration and type of KL. Effects of lignin incorporation on elongation at break (ε_{max}) of polymers were largely reported in the literature. As it can be seen in Figure 6a, samples containing ac-KL have a substantial decrease in elongation at break, probably due to lignin stiffness and the ac-KL tendency to form larger clusters, which might concentrate stresses and result in premature failures [1, 47]. On the other hand, the addition of alk-KL increased the elongation at break in low concentrations, which

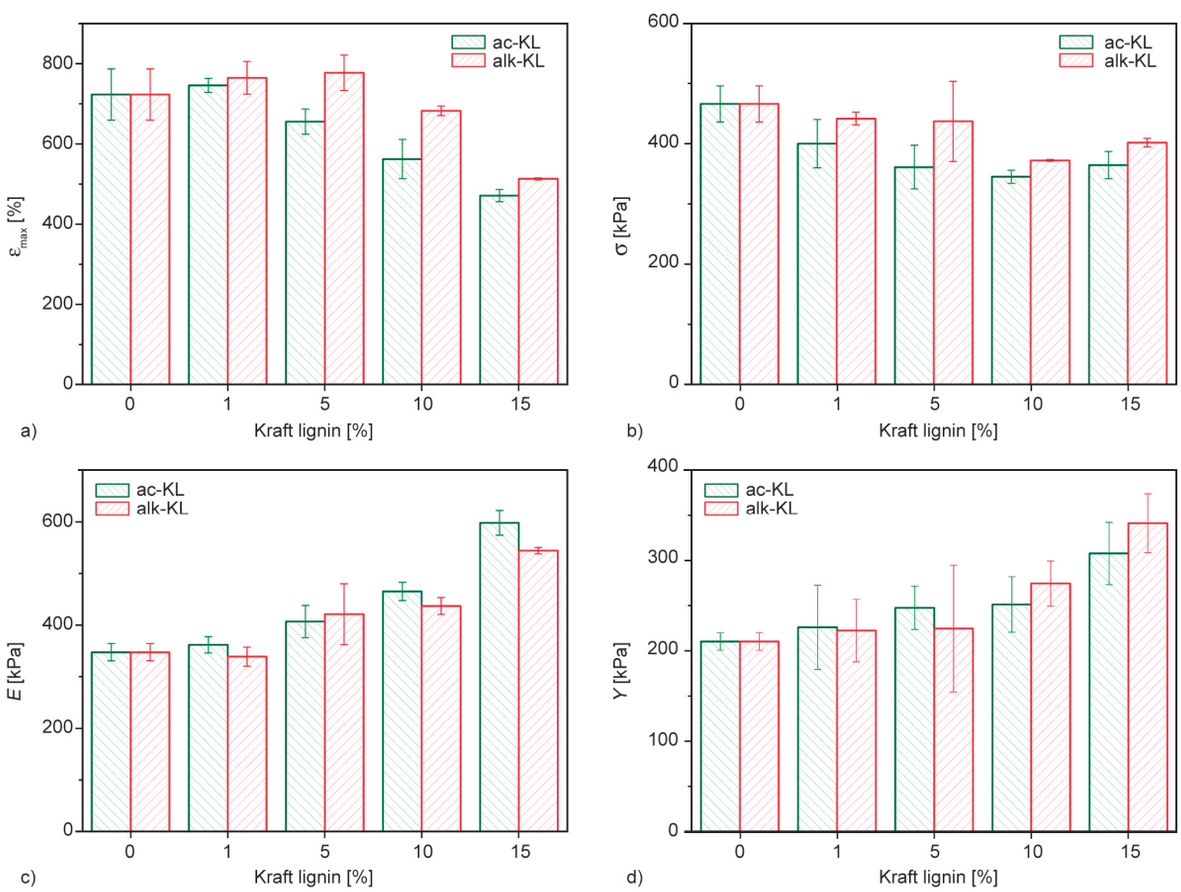

Figure 6. Average values of a) elongation at break (ε_{max}), b) maximum tensile strength (σ), and c) elastic moduli in tension (E) and d) compression (Y).

suggests stronger interactions between polymer phases as a result of adequate lignin dispersion [47, 48]. The alk-KL might act as physical cross-linking sites, similar to the PS block in the thermoplastic elastomer. At concentrations higher than 10% of alk-KL, small clusters were reported in the optical micrographs, leading to a decrease in the elongation at break.

Figure 6b shows a gradual decrease of maximum tensile strength (σ) as a result of increasing lignin concentration in the systems. This behavior has already been reported for several polymer systems, including polyolefin matrices [42, 49] and mixtures of lignin and polar polymers [42]. In our work, the values of tensile strength from samples containing alk-KL were less affected by lignin incorporation. This demonstrates a better balance between the mechanical properties resulting from the addition of alk-KL, attributed to its improved dispersion in the polymer matrix, in contrast to what was observed with the addition of ac-KL, where such balance is not achieved.

In contrast, elastic modulus (*E* – Figure 6c) was slightly increased by KL incorporation, corroborating DMA results. As previously mentioned, this behavior can be justified by the higher stiffness of KL, being observed in several lignin mixtures in different polymeric matrices [41, 42]. The same trend was observed for modulus obtained under compressive loading (*Y* – Figure 6d), which properly represents the mechanical loading in DEA applications during the electro-mechanical performance.

3.4. Dielectric properties

The relative permittivity of a material quantifies its ability to undergo polarization under an electric field. The real part (ε′) is known as the dielectric constant and is related to its charge values and stored energy, while the imaginary part (ε″) represents the dissipated energy, referred to as dielectric loss [15, 50].

Figure 7 presents the ε′ and ε″ values obtained through frequency sweep at room temperature for TPEGs with different types and concentrations of KL. The ε′ values of neat TPEG demonstrate a frequency-independent response, maintaining an average value of 2.4, characteristic of dielectrics with a low dipole moment [8, 51]. Overall, the inclusion of

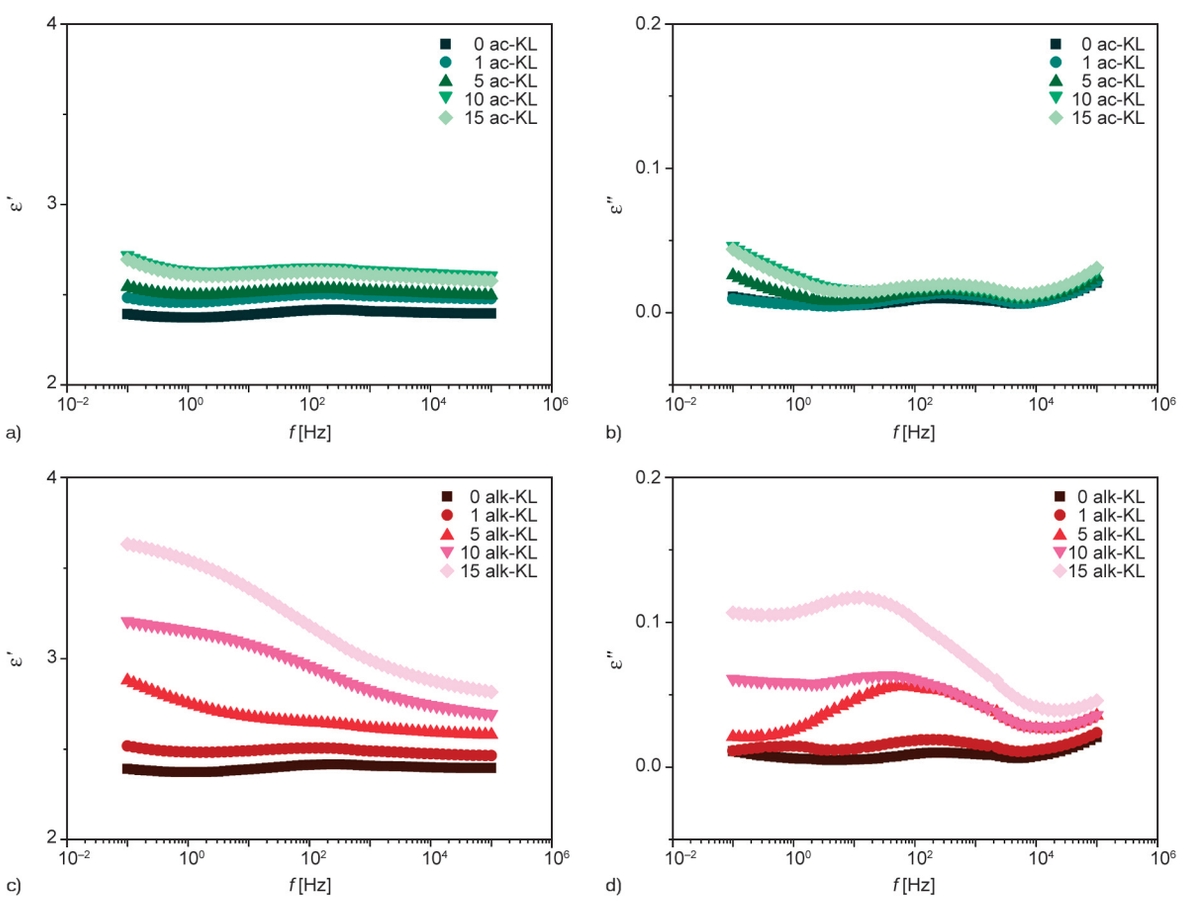

Figure 7. The real (ε′) and imaginary (ε″) parts of the relative permittivity of TPEG with a) and b) ac-KL and c) and d) alk-KL.

lignin resulted in an increased relative permittivity attributable to the polarization of its functional groups [52].

Khouaja *et al*. [51], when analyzing the dielectric behavior of polyethylene composites reinforced with cellulose or kraft fibers, observed a higher ε′ in samples with cellulose fibers, associating this with a higher concentration of hydroxyl groups compared to kraft fibers. It is noteworthy that, as indicated by the data in Table 2, each type of kraft lignin used has a different concentration of hydroxyl groups. Ac-KL possesses a slightly higher OH concentration (5.61 mmol/g) compared to alk-KL (5.14 mmol/g). Despite this, the relative permittivity is higher for the gels based on alk-KL. Additionally, each type of KL demonstrates a distinct behavior in terms of dielectric properties, suggesting that factors beyond OH content contribute to the polarization phenomena in the samples.

The addition of ac-KL resulted in an increase in ε′ of up to 12% in samples with 10 and 15 wt%, displaying a weak dependence on frequency (Figure 7a). This increase can be attributed to the electronic polarization of the ac-KL chain, originating from its polar groups [52]. On the other hand, in samples with the addition of alk-KL, a decrease in ε′ values with increasing frequency was observed (Figure 7c), a phenomenon known as dipolar relaxation [51]. This behavior can be explained by the challenge faced by dipoles in adjusting their orientation to rapid variations in the electric field at higher frequencies [50, 51]. At lower frequencies, in addition to electronic and dipolar polarizations, composite materials often exhibit a significant phenomenon of interfacial polarization, known as Maxwell/Wagner/Sillars (M/W/S) polarization [15, 51]. This interfacial polarization at low frequencies refers to the accumulation of free charges acting as dipoles at the interfaces or boundaries between the grains of materials composing a heterogeneous structure with polarity differences among its components. As the frequency increases, a significant reduction in interfacial and dipolar polarization is observed [51, 53, 54]. The addition of alk-KL led to a much more significant rise in ε′ (Figure 7c), showing a 51.7% increase in 15 alk-KL compared to the neat TPEG at a frequency of 10^{-1} Hz. Thus, the impact of KL dispersion on dielectric behavior is particularly notable in samples with alk-KL. The better dispersion of alk-KL, as observed in optical micrographs (Figure 3), induces the phenomenon of interfacial polarization in these composites, as there will be a greater number of contact interfaces in samples with alk-KL compared to those with ac-KL. This behavior aligns with findings reported by Helal *et al*. [15], who produced different SEBS/nanoclay nanocomposites and observed that samples with a more exfoliated morphology exhibited higher relative permittivity values. They attributed this effect to the greater number of nanoclay/polymer interfaces in the exfoliated form.

The results for ε″ in samples containing alk-KL (Figure 7d) reveal a relaxation shoulder around 10^2 Hz, associated with the relaxation of hydroxyl and methoxy groups present in the KL structure [55]. Although the same phenomenon is observed in ac-KL (Figure 7b), it manifests with less intensity, suggesting a limitation in the mobility and relaxation of KL due to the formation of more prominent aggregates. Additionally, a significant increase in ε″ is highlighted in the composite with alk-KL, characteristic of the interfacial polarization phenomenon [15, 51].

3.5. Electro-mechanical performance

Due to the previously discussed mechanical and dielectric properties, only the composites of TPEG with alk-KL were subjected to electro-mechanical actuation tests. The electro-mechanical performance of these samples under an electric field is presented in Figure 8.

To better assess the electro-mechanical actuation results, it is important to consider that, according to Equation (1), achieving enhanced electro-mechanical performance without the need for increased voltage requires materials with low elastic modulus and

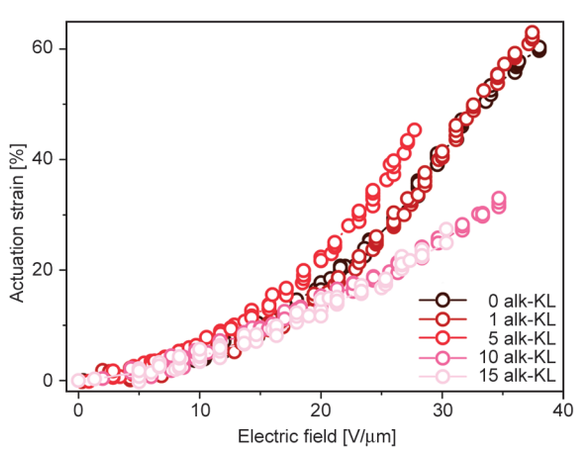

Figure 8. Experimental actuation strain as a function of electric field.

high relative permittivity, even though these properties are usually conflicting. While reducing thickness leads to an increase in the electric field, it can potentially lead to dielectric breakdown or electro-mechanical instability, thereby limiting the strain performance of the DEA. The ratio between relative permittivity and elastic modulus is known as electro-mechanical sensitivity and provides a figure of merit commonly used in multiphase materials, such as blends or nanocomposites [12, 56]. It assesses the electro-mechanical performance potential of the multiphase material (S_c) in comparison to the matrix (S_0), according to Equation (2):

$$F = \frac{S_c}{S_0} = \frac{\varepsilon'_c\, Y_0}{\varepsilon'_0\, Y_C} \tag{2}$$

where F is the electro-mechanical actuation potential, ε'_0 and Y_0 denote the relative permittivity and the compressive modulus of the pristine polymer gel, respectively, and ε'_c and Y_C refer to the same properties for the lignin-modified sample. Thus, the electro-mechanical performance potential provides a qualitative assessment of the electro-mechanical performance test. Samples with $F > 1$ will demonstrate an improvement in electro-mechanical performance over the polymer matrix. Table 4 presents the calculated values of F using the ε' values at a frequency of 1 kHz.

The sample 1 alk-KL showed no significant variation in comparison to the neat TPEG. Samples 10 and 15 alk-LK presented lower actuation strains in comparison to the TPEG. Although these samples have the highest values of relative permittivity, the increase in the compressive modulus overrides them, resulting in a reduction in electro-mechanical actuation. This is confirmed by the successive decrease in the value of F for 10 alk-KL (F = 0.90) and 15 alk-KL (F = 0.77).

Remarkably, the 5 alk-KL sample demonstrated a reduction in dielectric breakdown. While TPEG showed a dielectric breakdown in the order of 3 V/μm, this value was reduced to 27.7 V/μm for 5 alk-KL and 30.3 V/μm for 15 alk-KL. This effect of reduction in dielectric breakdown strength is common in multiphase materials [3]. In this case, lignin particles can act as centers of electrical defects that distort and increase the local field [57]. On the other hand, sample 5 alk-KL showed the highest value of electro-mechanical performance potential (F = 1.04) and, consequently, demonstrated greater electro-mechanical actuation capability. When comparing the values at an electric field of 27 V/μm, the 5 alk-KL sample exhibits an actuation strain of 43%, compared to 31% for TPEG and 21% for 15 alk-KL.

In summary, the results reveal the crucial influence of KL dispersion and concentration on the electro-mechanical and dielectric properties of the TPEG composite. The delicate balance between the relative permittivity and compressive modulus highlights the importance of carefully selecting materials for tailored applications. These findings offer a promising perspective for enhancing the performance of electro-mechanical systems in future technological applications.

Table 4. Values of electro-mechanical performance potential (F).

Sample	ε' (at 1 kHz)	F
0 alk-KL	2.41±0.02	–
1 alk-KL	2.49±0.03	0.97
5 alk-KL	2.67±0.01	1.04
10 alk-KL	2.82±0.02	0.90
15 alk-KL	2.99±0.02	0.77

4. Conclusions

This work demonstrates the potential of incorporating kraft lignin, particularly alkaline kraft lignin (alk-KL), to enhance the electro-mechanical performance of dielectric elastomers. The improved dispersion of alk-KL in the dielectric elastomer matrix resulted in a notable increase in the polymer's relative permittivity. This enhanced dispersibility of alk-KL, when compared to ac-KL, probably arises from the deprotonation of its structure during the isolation process.

Furthermore, the mechanical and viscoelastic properties remain essentially unaffected despite the addition of alk-KL up to a concentration of 5 wt%. As a result, when subjected to electro-mechanical actuation tests, the 5 alk-KL sample demonstrated a greater actuation strain under a relatively low electric field. This behavior is attributed to the improved ratio between the relative permittivity and compressive modulus, as illustrated by the electro-mechanical performance potential figure of merit.

In addition to the potential for improvement in electro-mechanical performance, the utilization of lignin demonstrates the capability to enhance dielectric properties, particularly important for insulating systems. Moreover, incorporating kraft lignin brings

environmental advantages to these systems. By re-utilizing this abundant byproduct of the pulp and paper industry, we not only enhance the performance of dielectric elastomers but also contribute to sustainable practices. This dual benefit underscores the significant potential of kraft lignin as a valuable reinforcement in the advancement and enhancement of dielectric elastomers applied as electroactive polymers.

Acknowledgements

The authors would like to thank the Multiuser Central Facilities (UFABC) for experimental support.

References

[1] de Sousa R. R., Heinze D. A., Sacramento J. B., Lanfredi A. J. C., Carastan D. J.: Electrical conductivity and *in situ* saxs probing of block copolymer nanocomposites under mechanical stretching. ACS Applied Materials and Interfaces, **15**, 27156–27165 (2023). https://doi.org/10.1021/acsami.3c03573

[2] Khan S. T., Mehdi M., Jamil T.: Electromechanical characterizations of PEDOT:PSS and its nanocomposite thin films on a cost-effective polymer substrate for microelectromechanical systems (MEMS) applications. Express Polymer Letters, **17**, 806–818 (2023). https://doi.org/10.3144/expresspolymlett.2023.60

[3] Romasanta L. J. J., Lopez-Manchado M. A. A., Verdejo R.: Increasing the performance of dielectric elastomer actuators: A review from the materials perspective. Progress in Polymer Science, **51**, 188–211 (2015). https://doi.org/10.1016/j.progpolymsci.2015.08.002

[4] Qiu Y., Zhang E., Plamthottam R., Pei Q.: Dielectric elastomer artificial muscle: Materials innovations and device explorations. Accounts of Chemical Research, **52**, 316–325 (2019). https://doi.org/10.1021/acs.accounts.8b00516

[5] Gu G-Y., Zhu J., Zhu L-M., Zhu X.: A survey on dielectric elastomer actuators for soft robots. Bioinspiration and Biomimetics, **12**, 1–22 (2017). https://doi.org/10.1088/1748-3190/12/1/011003

[6] Pelrine R., Kornbluh R., Pei Q., Joseph J.: High-speed electrically actuated elastomers with strain greater than 100%. Science, **287**, 836–839 (2000). https://doi.org/10.1126/science.287.5454.836

[7] Shankar R., Ghosh T. K., Spontak R. J.: Electroactive nanostructured polymers as tunable actuators. Advanced Materials, **19**, 2218–2223 (2007). https://doi.org/10.1002/adma.200602644

[8] de Sousa R. R., Carastan D. J.: Influence of morphology and rheological properties on the mechanical and dielectric behavior of block copolymer gels. Macromolecular Symposia, **383**, 1800056 (2019). https://doi.org/10.1002/masy.201800056

[9] Laurer J. H., Bukovnik R., Spontak R. J.: Morphological characteristics of SEBS thermoplastic elastomer gels. Macromolecules, **29**, 5760–5762 (1996). https://doi.org/10.1021/ma9607271

[10] Laurer J. H., Mulling J. F., Khan S. A., Spontak R. J., Bukovnik R.: Thermoplastic elastomer gels. I. Effects of composition and processing on morphology and gel behavior. Journal of Polymer Science Part B: Polymer Physics, **36**, 2379–2391 (1998). https://doi.org/10.1002/(SICI)1099-0488(19980930)36:13<2379::AID-POLB13>3.0.CO;2-0

[11] Chantawansri T. L., Duncan A. J., Ilavsky J., Stokes K. K., Berg M. C., Mrozek R. A., Lenhart J. L., Beyer F. L., Andzelm J. W.: Phase behavior of SEBS triblock copolymer gels. Journal of Polymer Science Part B: Polymer Physics, **49**, 1479–1491 (2011). https://doi.org/10.1002/polb.22335

[12] Bolados H. A., Hernández-Santana M., Romasanta L. J., Yazdani-Pedram M., Quijada R., López-Manchado M. A., Verdejo R.: Electro-mechanical actuation performance of SEBS/PU blends. Polymer, **171**, 25–33 (2019). https://doi.org/10.1016/j.polymer.2019.03.035

[13] Chen J-J., Qin S-H., Lv Q-C., Shi D-L., Zheng X-M., Wu H-J., Huang H-K., Lian L-G., He F-A., Lam K-H.: Preparation of novel xGNPs/SBS composites with enhanced dielectric constant and thermal conductivity. Advances in Polymer Technology, **37**, 1382–1389 (2018). https://doi.org/10.1002/adv.21797

[14] Grigorescu R. M., Ciuprina F., Ghioca P., Ghiurea M., Iancu L., Spurcaciu B., Panaitescu D. M.: Mechanical and dielectric properties of SEBS modified by graphite inclusion and composite interface. Journal of Physics and Chemistry of Solids, **89**, 97–106 (2016). https://doi.org/10.1016/j.jpcs.2015.10.008

[15] Helal E., Demarquette N. R., Amurin L. G., David E., Carastan D. J., Fréchette M.: Styrenic block copolymer-based nanocomposites: Implications of nanostructuration and nanofiller tailored dispersion on the dielectric properties. Polymer, **64**, 139–152 (2015). https://doi.org/10.1016/j.polymer.2015.03.026

[16] Helal E., David E., Fréchette M., Demarquette N. R.: Thermoplastic elastomer nanocomposites with controlled nanoparticles dispersion for HV insulation systems: Correlation between rheological, thermal, electrical and dielectric properties. European Polymer Journal, **94**, 68–86 (2017). https://doi.org/10.1016/j.eurpolymj.2017.06.038

[17] McCarthy D. N., Stoyanov H., Rychkov D., Ragusch H., Melzer M., Kofod G.: Increased permittivity nanocomposite dielectrics by controlled interfacial interactions. Composites Science and Technology, **72**, 731–736 (2012). https://doi.org/10.1016/j.compscitech.2012.01.026

[18] Romasanta L. J., Hernández M., López-Manchado M. A., Verdejo R.: Functionalised graphene sheets as effective high dielectric constant fillers. Nanoscale Research Letters, **6**, 508 (2011).
https://doi.org/10.1186/1556-276X-6-508

[19] Helal E., Amurin L. G., Carastan D. J., de Sousa R. R., David E., Fréchette M., Demarquette N. R.: Tuning the mechanical and dielectric properties of clay-containing thermoplastic elastomer nanocomposites. Polymer Engineering and Science, **58**, E174–E181 (2018).
https://doi.org/10.1002/pen.24844

[20] McCarthy D. N., Risse S., Katekomol P., Kofod G.: The effect of dispersion on the increased relative permittivity of TiO_2/SEBS composites. Journal of Physics D: Applied Physics, **42**, 145406 (2009).
https://doi.org/10.1088/0022-3727/42/14/145406

[21] Culebras M., Sanchis M. J., Beaucamp A., Carsí M., Kandola B. K., Horrocks A. R., Panzetti G., Birkinshaw C., Collins M. N.: Understanding the thermal and dielectric response of organosolv and modified kraft lignin as a carbon fibre precursor. Green Chemistry, **20**, 4461–4472 (2018).
https://doi.org/10.1039/C8GC01577E

[22] Gouveia J. R., da Costa C. L., Tavares L. B., dos Santos D. J.: Synthesis of lignin-based polyurethanes: A mini-review. Mini-Reviews in Organic Chemistry, **16**, 345–352 (2019).
https://doi.org/10.2174/1570193X15666180514125817

[23] Ponnusamy V. K., Nguyen D. D., Dharmaraja J., Shobana S., Banu J. R., Saratale R. G., Chang S. W., Kumar G.: A review on lignin structure, pretreatments, fermentation reactions and biorefinery potential. Bioresource Technology, **271**, 462–472 (2019).
https://doi.org/10.1016/j.biortech.2018.09.070

[24] Laurichesse S., Avérous L.: Chemical modification of lignins: Towards biobased polymers. Progress in Polymer Science, **39**, 1266–1290 (2014).
https://doi.org/10.1016/j.progpolymsci.2013.11.004

[25] Lupoi J. S., Singh S., Parthasarathi R., Simmons B. A., Henry R. J.: Recent innovations in analytical methods for the qualitative and quantitative assessment of lignin. Renewable and Sustainable Energy Reviews, **49**, 871–906 (2015).
https://doi.org/10.1016/j.rser.2015.04.091

[26] Ahvazi B., Cloutier É., Wojciechowicz O., Ngo T-D.: Lignin profiling: A guide for selecting appropriate lignins as precursors in biomaterials development. ACS Sustainable Chemistry and Engineering, **4**, 5090–5105 (2016).
https://doi.org/10.1021/acssuschemeng.6b00873

[27] Chakar F. S., Ragauskas A. J.: Review of current and future softwood kraft lignin process chemistry. Industrial Crops and Products, **20**, 131–141 (2004).
https://doi.org/10.1016/j.indcrop.2004.04.016

[28] Kai D., Tan M. J., Chee P. L., Chua Y. K., Yap Y. L., Loh X. J.: Towards lignin-based functional materials in a sustainable world. Green Chemistry, **18**, 1175–1200 (2016).
https://doi.org/10.1039/C5GC02616D

[29] Stiubianu G., Bele A., Tugui C., Musteata V.: New dielectric elastomers with improved properties for energy harvesting and actuation. in 'Proceedings for Advanced Topics in Optoelectronics, Microelectronics, and Nanotechnologies VII. Constanta, Romania' Vol. 9258, 925808 (2015).
https://doi.org/10.1117/12.2072287

[30] Zhang G., Tian C., Shi J., Zhang X., Liu J., Tan T., Zhang L.: Mechanically robust, self-repairable, shape memory and recyclable ionomeric elastomer composites with renewable lignin *via* interfacial metal–ligand Interactions. ACS Applied Materials and Interfaces, **14**, 38216–38227 (2022).
https://doi.org/10.1021/acsami.2c10731

[31] Carastan D. J., Vermogen A., Masenelli□Varlot K., Demarquette N. R.: Quantification of clay dispersion in nanocomposites of styrenic polymers. Polymer Engineering and Science, **50**, 257–267 (2010).
https://doi.org/10c.1002/pen.21527

[32] Antonino L. D., Gouveia J. R., de Sousa Júnior R. R., Garcia G. E. S., Gobbo L. C., Tavares L. B., dos Santos D. J.: Reactivity of aliphatic and phenolic hydroxyl groups in kraft lignin towards 4,4′ MDI. Molecules, **26**, 2131 (2021).
https://doi.org/10.3390/molecules26082131

[33] de Sousa R. R., Sacramento J. B., da Silva L. C. E., Becker D., Vidotti S. E., Carastan D. J.: High-performance block-copolymer-based dielectric elastomers with enhanced mechanical properties. ACS Applied Polymer Materials, **5**, 9505–9514 (2023).
https://doi.org/10.1021/acsapm.3c01880

[34] de Sousa Junior R. R., Gouveia J. R., Nacas A. M., Tavares L. B., Ito N. M., de Moura E. N., Gaia F. A., Pereira R. F., dos Santos D. J.: Improvement of polypropylene adhesion by kraft lignin incorporation. Materials Research, **22**, e20180123 (2019).
https://doi.org/10.1590/1980-5373-mr-2018-0123

[35] Tavares L. B., Ito N. M., Salvadori M. C., dos Santos D. J., Rosa D. S.: PBAT/kraft lignin blend in flexible laminated food packaging: Peeling resistance and thermal degradability. Polymer Testing, **67**, 169–176 (2018).
https://doi.org/10.1016/j.polymertesting.2018.03.004

[36] Barzegari M. R., Alemdar A., Zhang Y., Rodrigue D.: Mechanical and rheological behavior of highly filled polystyrene with lignin. Polymer Composites, **33**, 353–361 (2012).
https://doi.org/10.1002/pc.22154

[37] Pouteau C., Baumberger S., Cathala B., Dole P.: Lignin–polymer blends: Evaluation of compatibility by image analysis. Comptes Rendus Biologies, **327**, 935–943 (2004).
https://doi.org/10.1016/j.crvi.2004.08.008

[38] Hubbe M., Alén R., Paleologou M., Kannangara M., Kihlman J.: Lignin recovery from spent alkaline pulping liquors using acidification, membrane separation, and related processing steps: A review. BioResources, **14**, 2300–2351 (2019). https://doi.org/10.15376/biores.14.1.2300-2351

[39] Ela R. C. A., Spahn L., Safaie N., Ferrier R. C., Ong R. G.: Understanding the effect of precipitation process variables on hardwood lignin characteristics and recovery from black liquor. ACS Sustainable Chemistry and Engineering, **8**, 13997–14005 (2020). https://doi.org/10.1021/acssuschemeng.0c03692

[40] Kienberger M., Maitz S., Pichler T., Demmelmayer P.: Systematic review on isolation processes for technical lignin. Processes, **9**, 804 (2021). https://doi.org/10.3390/pr9050804

[41] Kun D., Pukánszky B.: Polymer/lignin blends: Interactions, properties, applications. European Polymer Journal, **93**, 618–641 (2017). https://doi.org/10.1016/j.eurpolymj.2017.04.035

[42] Romhányi V., Kun D., Pukánszky B.: Correlations among miscibility, structure, and properties in thermoplastic polymer/lignin blends. ACS Sustainable Chemistry and Engineering, **6**, 14323–14331 (2018). https://doi.org/10.1021/acssuschemeng.8b02989

[43] Rath T., Li Y.: Nanocomposites based on polystyrene-*b*-poly(ethylene-*r*-butylene)-*b*-polystyrene and exfoliated graphite nanoplates: Effect of nanoplatelet loading on morphology and mechanical properties. Composites Part A: Applied Science and Manufacturing, **42**, 1995–2002 (2011). https://doi.org/10.1016/j.compositesa.2011.09.002

[44] Tse M. F.: Studies of triblock copolymer-tackifying resin interactions by viscoelasticity and adhesive performance. Journal of Adhesion Science and Technology, **3**, 551–570 (1989). https://doi.org/10.1163/156856189X00407

[45] Seitz M. E., Burghardt W. R., Faber K. T., Shull K. R.: Self-assembly and stress relaxation in acrylic triblock copolymer gels. Macromolecules, **40**, 1218–1226 (2007). https://doi.org/10.1021/ma061993+

[46] de Sousa Júnior R. R., Garcia G. E. S., dos Santos D. J., Carastan D. J.: Viscoelastic behavior of pressure-sensitive adhesive based on block copolymer and kraft lignin. The Journal of Adhesion, **100**, 139–155 (2023). https://doi.org/10.1080/00218464.2023.2201443

[47] Bahl K., Swanson N., Pugh C., Jana S. C.: Polybutadiene-*g*-polypentafluorostyrene as a coupling agent for lignin-filled rubber compounds. Polymer, **55**, 6754–6763 (2014). https://doi.org/10.1016/j.polymer.2014.11.008

[48] Tran C. D., Chen J., Keum J. K., Naskar A. K.: A new class of renewable thermoplastics with extraordinary performance from nanostructured lignin-elastomers. Advanced Functional Materials, **26**, 2677–2685 (2016). https://doi.org/10.1002/adfm.201504990

[49] Bozsódi B., Romhányi V., Pataki P., Kun D., Renner K., Pukánszky B.: Modification of interactions in polypropylene/lignosulfonate blends. Materials and Design, **103**, 32–39 (2016). https://doi.org/10.1016/j.matdes.2016.04.061

[50] Wang Q., Che J., Wu W., Hu Z., Liu X., Ren T., Chen Y., Zhang J.: Contributing factors of dielectric properties for polymer matrix composites. Polymers, **15**, 590 (2023). https://doi.org/10.3390/polym15030590

[51] Khouaja A., Koubaa A., Daly H. B.: Dielectric properties and thermal stability of cellulose high-density polyethylene bio-based composites. Industrial Crops and Products, **171**, 113928 (2021). https://doi.org/10.1016/j.indcrop.2021.113928

[52] Bogolitsyn K. G., Khviyuzov S. S., Volkov A. S., Koposov G. D., Gusakova M. A.: Broadband dielectric spectroscopy of lignin. Russian Journal of Physical Chemistry A, **93**, 353–358 (2019). https://doi.org/10.1134/S0036024419020055

[53] Dakin T. W.: Conduction and polarization mechanisms and trends in dielectric. IEEE Electrical Insulation Magazine, **22**, 11–28 (2006). https://doi.org/10.1109/MEI.2006.1705854

[54] Anjeline J. C., Mali D. P., Lakshminarasimhan N.: High dielectric constant of $NiFe_2O_4$–$LaFeO_3$ nanocomposite: Interfacial conduction and dielectric loss. Ceramics International, **47**, 34278–34288 (2021). https://doi.org/10.1016/j.ceramint.2021.08.338

[55] Khviyuzov S., Bogolitsyn K., Volkov A., Koposov G., Gusakova M.: Features of frequency dependence of electrical conductivity and dielectric properties in lignins from conifers and deciduous trees. Holzforschung, **74**, 1113–1122 (2020). https://doi.org/10.1515/hf-2019-0149

[56] Romasanta L. J., Leret P., Casaban L., Hernández M., de la Rubia M. A., Fernández J. F., Kenny J. M., Lopez-Manchado M. A., Verdejo R.: Towards materials with enhanced electro-mechanical response: $CaCu_3Ti_4O_{12}$–polydimethylsiloxane composites. Journal of Materials Chemistry, **22**, 24705 (2012). https://doi.org/10.1039/c2jm34674e

[57] Yan J., Yan S., Tilly J. C., Ko Y., Lee B., Spontak R. J.: Ionic complexation of endblock-sulfonated thermoplastic elastomers and their physical gels for improved thermomechanical performance. Journal of Colloid and Interface Science, **567**, 419–428 (2020). https://doi.org/10.1016/j.jcis.2020.02.007